*Int. J. Oral Maxillofac. Surg. 2006; 35: 551–555*
doi:10.1016/j.ijom.2005.12.007, available online at http://www.sciencedirect.com

International Journal of
Oral & Maxillofacial Surgery

Technical Note
Congenital Craniofacial Anomalies

# Alveolar cleft osteoplasty using tissue-engineered osteogenic material

**H. Hibi[1], Y. Yamada[2], M. Ueda[2], Y. Endo[2]**
[1]Center for Genetic and Regenerative Medicine, Nagoya University School of Medicine, Nagoya, Japan; [2]Department of Oral and Maxillofacial Surgery, Nagoya University Graduate School of Medicine, Nagoya, Japan

*H. Hibi, Y. Yamada, M. Ueda, Y. Endo: Alveolar cleft osteoplasty using tissue-engineered osteogenic material. Int. J. Oral Maxillofac. Surg. 2006; 35: 551–555.*


*Abstract.* The use of tissue-engineered osteogenic material comprising platelet-rich plasma and autologous mesenchymal stem cells isolated, expanded and induced to osteogenic potential in bone augmentation procedures as a replacement for autologous bone grafts, offers predictable results with minimal donor-site morbidity. This material was applied for an alveolar cleft osteoplasty of a 9-year-old female patient. Serial computed tomograms showed the regenerated bone extending from the cleft walls after 3 months and bridging the cleft after 6 months, with 79.1% of the grafted region after 9 months at the time when the canine and lateral incisor in the affected side erupted in the reconstructed alveolar ridge.

Accepted for publication 16 December 2005
Available online 11 April 2006

The reconstruction of alveolar cleft defects is well established, with the most widely accepted approach being secondary alveolar cleft osteoplasty in the mixed dentition phase with autologous bone grafting[4,18]. The source material for most bone grafts has been particulate marrow harvested from the anterior iliac crest, and this represents the standard material with which other materials from rib, mandible, calvarium, and tibia are compared[2,4,18]. Donor-site morbidity is an important factor in deciding the site for harvesting cancellous bone. Allogenic or xenogenic materials can eliminate this concern but not the risk of disease transmission. Osteoinductive agents such as recombinant human bone morphogenetic protein-2[1,5,7] can solve these problems and are expected to be used clinically in the future. As another solution, the use of tissue-engineered osteogenic material (TEOM) comprising autologous mesenchymal stem cells (MSCs) and platelet-rich plasma (PRP) in bone augmentation procedures as a replacement for autologous bone grafts, offers predictable results with minimal donor-site morbidity[3,16]. Here we report a technique and case of alveolar cleft osteoplasty using TEOM as a translational research.

## Patient and method

### Case description

A 3-month-old female patient born with a congenital left unilateral cleft lip and alveolus underwent a cheiloplasty at that had resulted in no remaining oronasal fistula. At 9 years of age, computed tomograms (CTs) revealed that the left maxillary canine, lateral, and supernumerary incisors had formed half of their roots, and that they closely surrounded the alveolar cleft bony defect which was 10 mm wide and 13 mm deep anteroposteriorly (Fig. 1). The left central incisor was orthodontically overcorrected due to previous severe rotation and distal location. When secondary alveolar cleft osteoplasty was indicated, the patient and her parents were informed about the nature of the TEOM, and they granted their consent.

### Tissue-engineered osteogenic material

The clinical protocol as a translational research of TEOM was approved by the ethics committee of Nagoya University. Autologous blood (200 ml) was harvested

0901-5027/060551 + 05 $30.00/0 

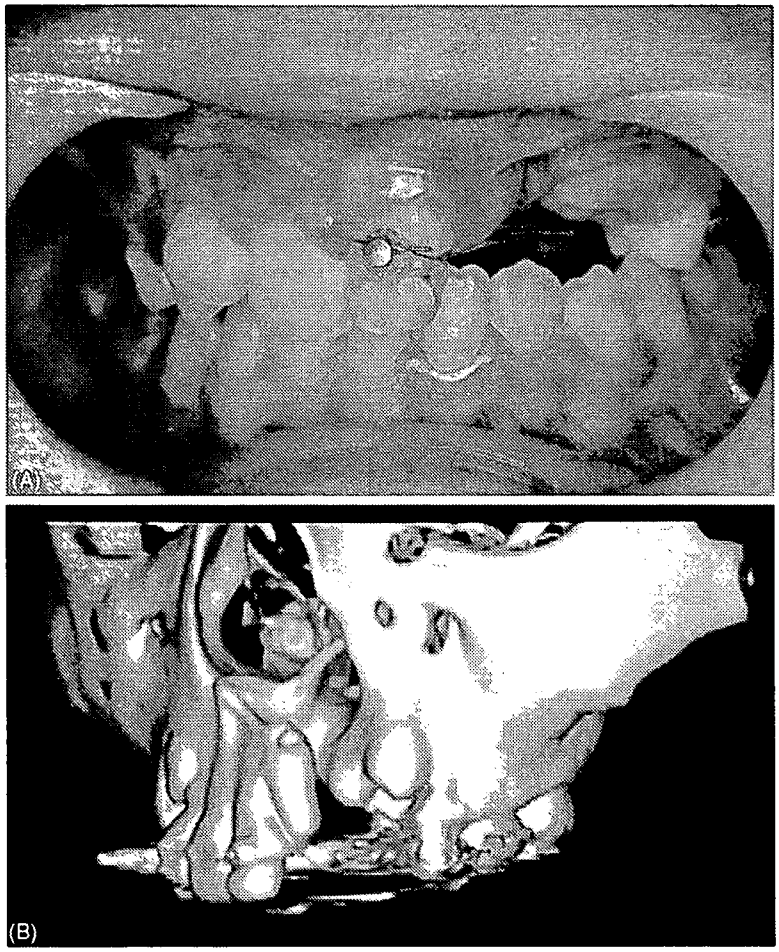


*Fig. 1.* The left unilateral cleft of the alveolus of our 9-year-old female patient: (A) intraoral view; and (B) 3-dimensional computed tomogram demonstrating the left maxillary canine and the alveolar bony defect.

three times every 2 weeks to extract serum (100 ml) and 300 ml of serum was cryopreserved. Approximately 10 ml of the bone marrow aspirate was collected from the anterior iliac crest with a 14-gauge biopsy needle under local anesthesia. The aspirating procedure did not cause any additional discomfort to the patient. The MSCs were isolated from the marrow aspirates and cultured as reported previously[10,16]. The cells were suspended in a low-glucose Dulbecco's modified Eagle's medium containing L-glutamine, penicillin and streptomycin (Cambrex, Walkersville, MD), and supplemented with the 15% autologous serum and incubated at 37 °C in a humidified atmosphere containing 95% air and 5% $CO_2$. The MSCs were replated and expanded for 4 weeks, and then induced to osteogenic potential for another week with 100 nM dexamethasone, 10 mM β-glycerophosphate and 50 μg/ml ascorbic acid-2-phosphate (Sigma-Aldrich, St. Louis, MO). The differentiated MSCs were confirmed by detecting alkaline phosphatase activity. Approximately 10 ml of PRP was extracted from 100 ml of autologous blood using centrifugation and a selective collection technique[6,16] 1 day before the surgery and contained $8.9 \times 10^5$ platelets/μl (i.e. 313 % higher than the original whole blood). During the operation, $5.0 \times 10^7$ differentiated MSCs, 1.8 ml of the PRP, 0.3 ml of 10% calcium chloride solution containing 300 units of human thrombin and 0.3 ml of air were mixed and polymerized into a gel form of the TEOM.

### Operative technique

Following a 3-cm-long mucosal incision at the level of the labiogingival junction, dissections were made in the ingrown scar tissue to reach the bony surface of the cleft walls. The tissue was then elevated in the subperiosteal plane to the levels of the anterior nasal spine anteriorly, the lateral piriform rim superiorly and to the alveolar ridges inferiorly, whilst taking care not to damage the unerupted teeth and the content of the incisive canal. The flaps of the nasal floor and the oral mucosa formed the ceiling and the floor of the cleft cavity, respectively. The ceiling, floor and front walls of the defect were supported with a 0.1-mm-thick titanium-mesh plate (Stryker, Kalamazoo, MI). The thus-created pouch was filled with all the prepared TEOM through a syringe using a packer (Fig. 2). Following release incisions in the periosteum and the scar tissue of the flaps and to allow them to cover the grafted area, the wound was consequently closed without tension.

### Postoperative course

The patient exhibited an uneventful postoperative course. The radiopacity of serial CTs slicing the middle level of the alveolar cleft in the grafted region increased gradually over the time (Fig. 3). Dome-shaped radiopaque images with 233 Hounsfield units (HU) faced together and extended from the cleft bony walls inside the cavity after 3 months, and were fused together into an image with 324 HU after 6 months. The image increased in radiopacity to 447 HU in 9 months, and at the bony bridge the lateral and supernumerary incisors horizontally approximated from their original positions in the respective major and minor segments. The incisive canal was reconstructed just medial to the bridge. The erupting canine and lateral incisor pushed the mesh plate vertically, and the mucosa covering the cleft consequently swelled and thinned. A mucosal cut was made in the crest of the alveolar ridge over these teeth, and the part of the plate overlying the teeth was removed under local anesthesia. The canine and the lateral incisor then erupted approximately at the same time (Fig. 4).

## Discussion

Cells, cytokines and a matrix are three prerequisites for tissue engineering[8,9,10,15], and MSCs and PRP compounds were applied in the present TEOM. The PRP contains not only fibrinogen that forms a fibrin network acting as a matrix but also chemical substances such as platelet-derived growth factor, transforming growth factor-β, vascular endothelial growth factor, and insulin-like growth factor. These factors contribute to cellular proliferation, matrix formation, collagen synthesis, osteoid production, and other processes that accelerate tissue regeneration[6].

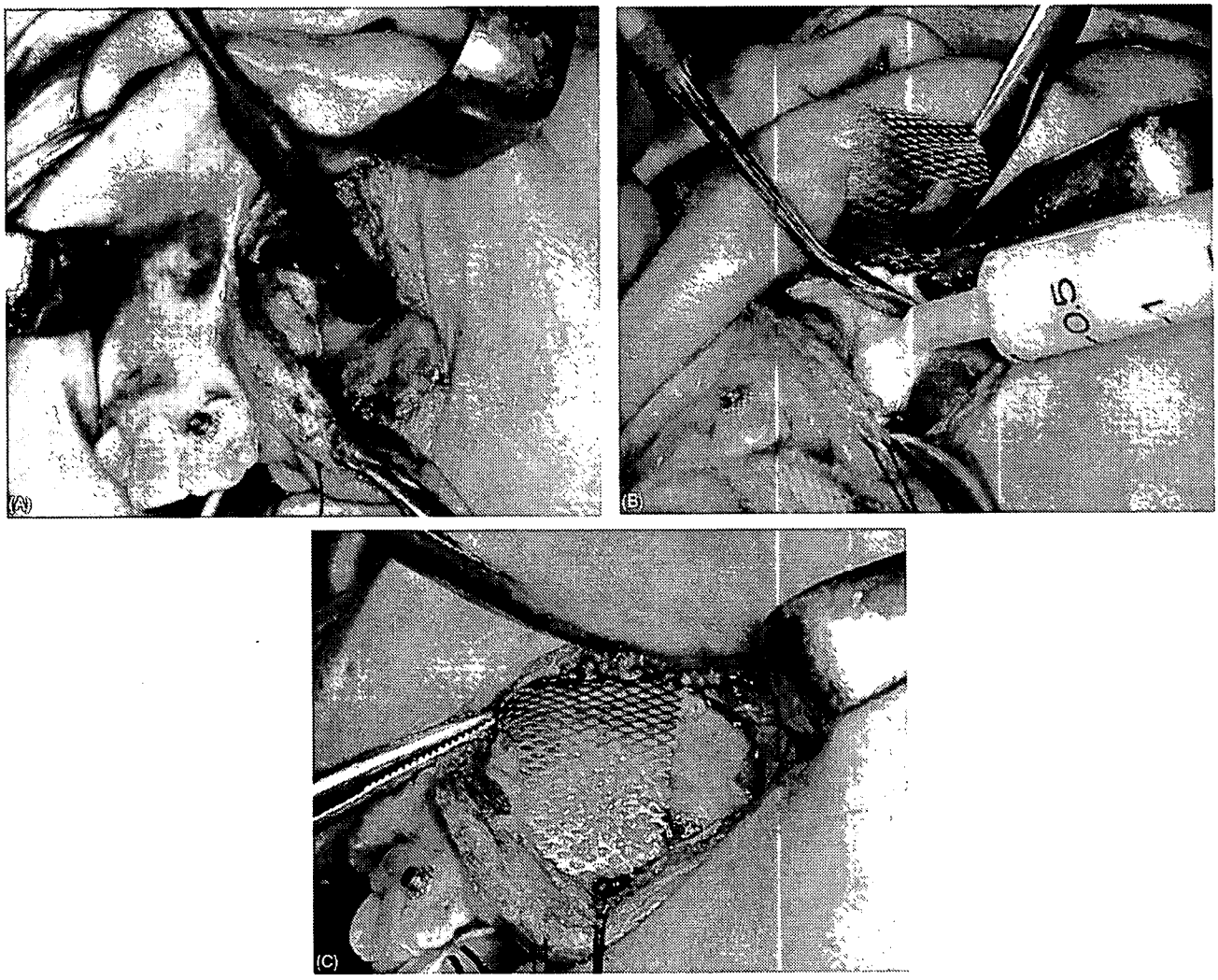


*Fig. 2.* Intraoperative views: (A) exposed alveolar cleft defect; (B) cleft cavity grafted with the tissue-engineered osteogenic material; and (C) graft covered with the titanium mesh plate.

TEOM regenerated the bone in the alveolar cleft defect without donor-site morbidity resulting from the autologous bone graft. Grafted bone remodels new bone due to apposition following resorption, and VAN DER MEIJ et al.[13] reported that 1-year postoperative volumetric rates were approximately 70% for secondary bone grafts before canine eruption. Using their measuring method[13] at 9 months postoperatively the present case showed 79.1% regenerated bone. They also stated that the eruption of the canine generally occurred 2 years after bone graft if the patient was 9-years-old. A high resorbability of the bone in the grafted region may result in the early eruption of canine. In the present case the canine coronally forced the mesh plate at 9 months postoperatively, which was earlier than expected. As the bone regenerated in the cleft defect, the ingrowing bone seemed to accompany the roots of not only the canine but also the lateral and supernumerary incisors, which consequently approximated and erupted. Bone regeneration with the TEOM may therefore, have helped to induce teeth to reposition properly in the horizontal and vertical planes.

The mucoperiosteal flaps require the support in proper reconstruction of alveolar morphology, and hence the TIME technique[14] was indicated for the present simple cleft without palatal defect or oronasal fistula. The titanium mesh plate facilitated a rigid space without disturbing the blood supply from the overlying flaps, but needed to be removed before tooth eruption. Resorbable membranes solve this problem but inhibit the blood supply. The skeletal frame or carriers of biodegradable material such as polylactide polymer or collagen may serve as another solution[11,12].

Distraction of the transport bony segment has been attempted for closing alveolar defects[17]. The defects are actually only reduced and not eliminated, and the teeth in the transport segment also moved unintentionally according to the distraction. Some alteration in teeth positions may be beneficial, but others compromise crown morphology or require its recontouring. The bone transport in repair of the alveolar cleft therefore remains controversial.

The TEOM thus shows promise with further perspectives. Younger patients have more MSCs, and their harvesting, isolation and cryopreservation allows TEOM to be supplied repeatedly when needed. This repeatability will facilitate the sequential treatments of cleft patients in the future.

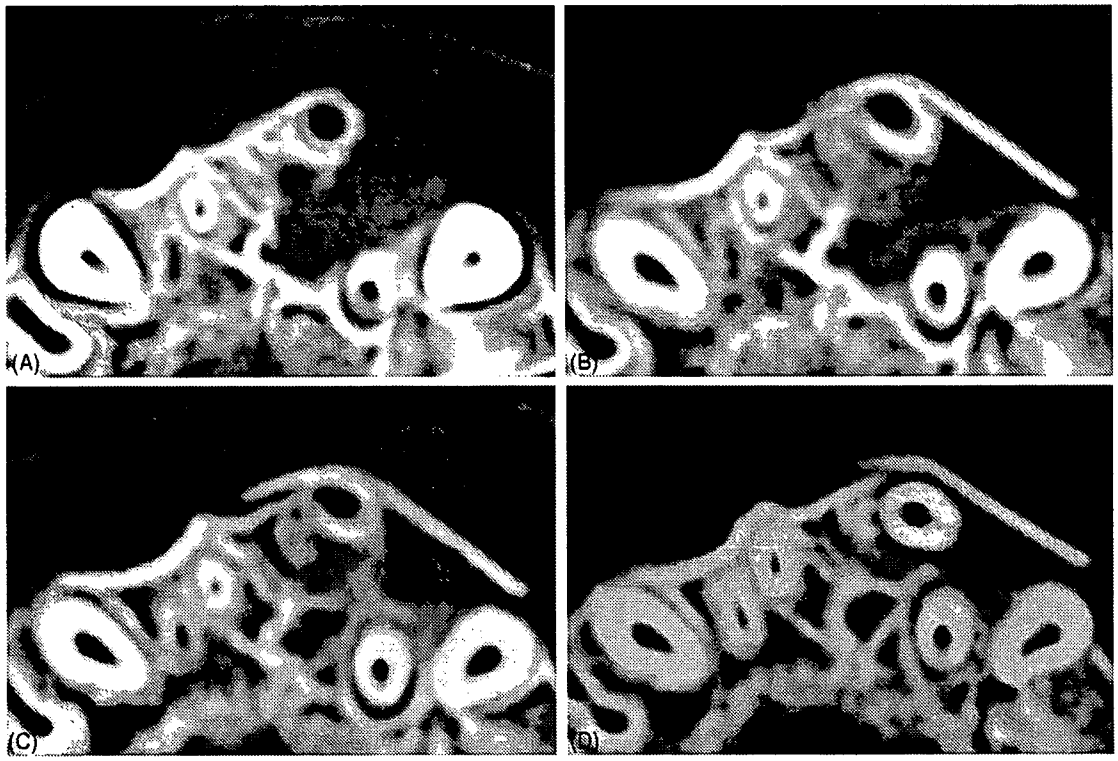


*Fig. 3.* Serial computed tomograms slicing the middle level of the alveolar cleft: (A) preoperation; (B) 3 months postoperation. Dome-shaped radiopaque images facing together and extending from the cleft bony walls inside the cavity (C) 6 months postoperation. Fused image in the cleft cavity and (D) 9 months postoperation. The lateral and supernumerary incisors are approximated in the bony bridge lateral to the reconstructed incisive canal.

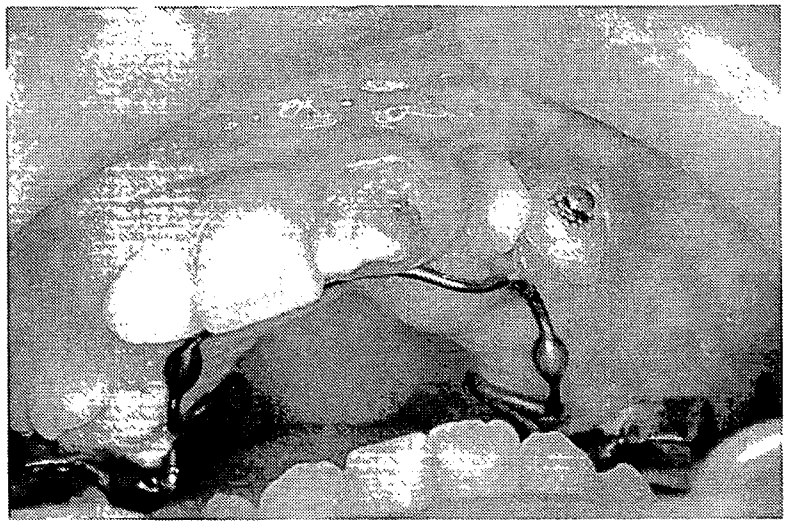

*Fig. 4.* The canine and the lateral incisor erupting in the reconstructed alveolar ridge.

*Acknowledgements.* This research was partially supported by the Ministry of Education, Culture, Sports, Science and Technology, Japan. The authors acknowledge with thanks the technical support of OsteoGenesis Inc., Japan.

## References

1. Boyne PJ, Nath R, Nakamura A. Human recombinant BMP-2 in osseous reconstruction of simulated cleft palate defects. Br J Oral Maxillofac Surg 1998: **36**: 84–90.
2. Fonseca RJ, Turvey TA, Wolford LM. Orthognathic surgery in the cleft patients. In: Fonseca RJ, ed: Oral and Maxillofacial Surgery, Vol. 6, Cleft/craniofacial/cosmetic surgery. Philadelphia: W.B. Saunders 2000: 87–146.
3. Hibi H, Yamada Y, Kagami H, Ueda M. Distraction osteogenesis assisted by tissue engineering in an irradiated mandible: a case report. Int J Oral Maxillofac Implants 2006: **21**: 141–147.
4. Horswell BB, Henderson JM. Secondary osteoplasty of the alveolar cleft defect. J Oral Maxillofac Surg 2003: **61**: 1082–1090.
5. Kawamoto T, Motohashi N, Kitamura A, Baba Y, Suzuki S, Kuroda T. Experimental tooth movement into bone induced by recombinant human bone morphogenetic protein-2. Cleft Palate Craniofac J 2003: **40**: 538–543.
6. Marx RE, Garg AK. Dental and Craniofacial Application of Platelet-rich Plasma. Illinois: Quintessence Publishing 2005: pp. 1–168.
7. Mayer M, Hollinger J, Ron E, Wozney J. Maxillary alveolar cleft repair in dogs using recombinant human bone morphogenetic protein-2 and a polymer carrier. Plast Reconstr Surg 1996: **98**: 247–259.
8. Meyer U, Joos U, Wiesmann HP. Biological and biophysical principles in

extracorporal bone tissue engineering. Part I. Int J Oral Maxillofac Surg 2004: **33**: 325–332.
9. MEYER U, JOOS U, WIESMANN HP. Biological and biophysical principles in extracorporal bone tissue engineering. Part III. Int J Oral Maxillofac Surg 2004: **33**: 635–641.
10. PITTENGER MF, MACKAY AM, BECK SC, JAISWAL RK, DOUGLAS R, MOSCA JD, MOORMAN MA, SIMONETTI DW, CRAIG S, MARSHAK DR. Multilineage potential of adult human mesenchymal stem cells. Science 1999: **284**: 143–147.
11. SCHMELZEISEN R, SCHIMMING R, SITTINGER M. Making bone: implant insertion into tissue-engineered bone for maxillary sinus floor augmentation – a preliminary report. J Cranio-Maxillofac Surg 2003: **31**: 34–39.
12. SCHIMMING R, SCHMELZEISEN R. Tissue-engineered bone for maxillary sinus augmentation. J Oral Maxillofac Surg 2004: **62**: 724–729.
13. VAN DER MEIJ AJW, BAART JA, PRAHL-ANDERSEN B, VALK J, KOSTENSE PJ, TUINZING DB. Bone volume after secondary bone grafting in unilateral and bilateral clefts determined by computed tomography scans. Oral Surg Oral Med Oral Pathol Oral Radiol Endod 2001: **92**: 136–141.
14. VON ARX T, HARDT N, WALLKAMM B. The TIME technique: a new method for localized alveolar ridge augmentation prior to placement of dental implants. Int J Oral Maxillofac Implants 1996: **11**: 387–394.
15. WIESMANN HP, JOOS U, MEYER U. Biological and biophysical principles in extracorporal bone tissue engineering. Part II. Int J Oral Maxillofac Surg 2004: **33**: 523–530.
16. YAMADA Y, UEDA M, HIBI H, NAGASAKA T. Translational research for injectable tissue-engineered bone regeneration using mesenchymal stem cells and platelet-rich plasma: from basic research to clinical case study. Cell Transplant 2004: **13**: 343–355.
17. YEN SL-K, YAMASHITA DD, GROSS J, MEARA JG, YAMAZAKI K, KIM TH, REINISCH J. Combining orthodontic tooth movement with distraction osteogenesis to close cleft spaces and improve maxillary arch form in cleft lip and palate patients. Am J Orthod Dentofacial Orthop 2005: **127**: 224–232.
18. ZEITLER D. Alveolar cleft grafts. In: FONSECA RJ, ed: Oral and Maxillofacial Surgery, Vol. 6 Cleft/ craniofacial/cosmetic surgery. Philadelphia: W.B. Saunders 2000: 75–86.

Address:
*Hideharu Hibi,*
*Center for Genetic and Regenerative Medicine*
*Nagoya University School of Medicine*
*65 Tsurumai-cho*
*Showa-ku*
*Nagoya 466-8560*
*Japan*
*Tel: +81 52 7442348*
*Fax: +81 52 7442352*
*E-mail: hibihi@med.nagoya-u.ac.jp*

RESEARCH REPORTS
Biomaterials & Bioengineering

H. Agata[1,2], I. Asahina[3]*, Y. Yamazaki[4], M. Uchida[1], Y. Shinohara[1], M.J. Honda[1], H. Kagami[1], and M. Ueda[1,2]

[1]Division of Stem Cell Engineering, The Institute of Medical Science, The University of Tokyo, Tokyo, Japan; [2]Department of Oral and Maxillofacial Surgery, Nagoya University Graduate School of Medicine, Nagoya, Japan; [3]Department of Regenerative Oral Surgery, Nagasaki University Graduate School of Biomedical Sciences, Nagasaki, Japan; and [4]Department of Plastic and Reconstructive Surgery, Kitasato University School of Medicine, Kanagawa, Japan; *corresponding author, 1-7-1 Sakamoto, Nagasaki 852-8588, Japan, asahina@nagasaki-u.ac.jp

*J Dent Res* 86(1):79-83, 2007

# Effective Bone Engineering with Periosteum-derived Cells

## ABSTRACT

Bone augmentation *via* tissue engineering has generated significant interest. We hypothesized that periosteum-derived cells could be used in place of bone marrow stromal cells (which are widely used) in bone engineering, but the differences in osteogenic potential between these 2 cell types are unclear. Here, we compared the osteogenic potential of these cells, and investigated the optimal osteoinductive conditions for periosteum-derived cells. Both cell types were induced, *via* bFGF and BMP-2, to differentiate into osteoblasts. Periosteal cells proliferated faster than marrow stromal cells, and osteogenic markers indicated that bone marrow stromal cells were more osteogenic than periosteal cells. However, pre-treatment with bFGF made periosteal cells more sensitive to BMP-2 and more osteogenic. Transplants of periosteal cells treated with BMP-2 after pre-treatment with bFGF formed more new bone than did marrow stromal cells. Analysis of these data suggests that combined treatment with bFGF and BMP-2 can make periosteum a highly useful source of bone regeneration.

**KEY WORDS:** marrow stromal cells, periosteal cells, osteogenic potential, bFGF, BMP-2.

Received February 21, 2006; Last revision September 8, 2006; Accepted September 26, 2006

## INTRODUCTION

Bone defects that do not heal spontaneously need bone reconstruction for the recovery of bone function. While autografting is the gold standard in bone reconstructive surgery, autografts involve donor site morbidity. Artificial bone substitutes are also utilized; however, results are inconsistent, because these materials lack osteogenic potential. Recently, tissue engineering has attracted considerable attention (Young *et al.*, 2005). Because it requires only a small amount of tissue from the patient, bone reconstruction by this technique is less invasive and is safer than conventional methods. Bone marrow stromal cells have multi-lineage differentiation potential and can therefore differentiate into cells with an osteogenic phenotype. Accordingly, they have been frequently used for bone reconstruction (Luria *et al.*, 1987; Haynesworth *et al.*, 1992; Matsubara *et al.*, 2005). Periosteum-derived cells have also been used recently (Breitbart *et al.*, 1998; Perka *et al.*, 2000). There is a growing requirement for dentists to regenerate alveolar bone as a regenerative therapy for periodontitis and in implant dentistry. Concerning the donor site, it is easier for general dentists to harvest periosteum than marrow stromal cells, because they can access the mandibular periosteum during routine oral surgery. However, the differences in osteogenic potential between marrow stromal cells and periosteal cells remain unclear. In the present study, we compared the osteogenic potential of periosteum-derived cells and marrow stromal cells, after treatment with basic fibroblast growth factor (bFGF) and bone morphogenetic protein-2 (BMP-2), both of which have significant effects on osteogenesis (Rosen and Thies, 1992; Marie, 2003). Recently, Fakhry *et al.* (2005) showed that the combined use of bFGF and BMP-2 greatly enhances the osteogenic potential of chick embryonic calvaria-derived cells. Therefore, using BMP-2 and bFGF under the conditions described by Fakhry, with modifications, we attempted to determine the optimal osteo-inductive conditions for human mandibular periosteum-derived cells.

## MATERIALS & METHODS

### Cell Cultures

The study conformed to the tenets of the Declaration of Helsinki, and the protocol was approved by the Ethical Committees of both Kitasato University and the Institute of Medical Science, The University of Tokyo. All subjects provided written informed consent.

Human periosteal tissue (1 $cm^2$) was obtained from the mandibular angle of six patients (ages [yrs] 18, 19, 20, 21, 21, 24; gender, one male and five females) during the course of oral surgery. The excised sections of tissue were plated into 10-cm dishes (TPP, Zollstrasse, Trasadingen, Switzerland) containing α-MEM (Kohjin Bio, Saitama, Japan), supplemented with 10% fetal bovine serum (JRH Bioscience, Lenexa, KS, USA) and 1% penicillin-streptomycin-glutamine (serum-conditioned α-MEM, Invitrogen, Carlsbad, CA, USA), and were

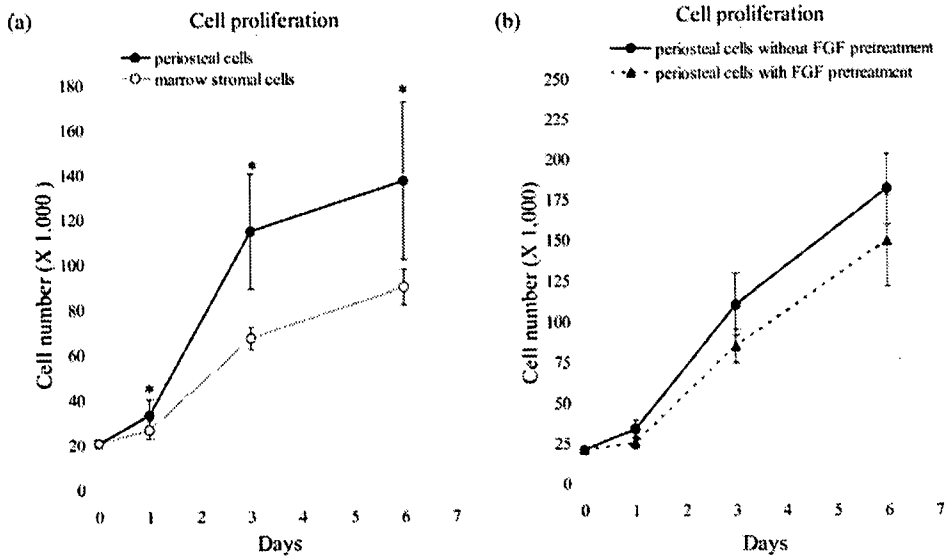


**Figure 1.** Periosteal cells (closed circles) and marrow stromal cells (open circles) were plated in 12-well plates at a density of 2.0 x $10^4$ cells/well. Cell numbers were counted directly (**a**). FGF-pre-treated periosteal cells are indicated by closed triangles, and non-pre-treated periosteal cells are indicated by closed circles (**b**). Values are means ± standard deviation for 3 cultures. Asterisk indicates significant difference in the number of periosteal cells, compared with marrow stromal cells on the same day; $p < 0.05$.

cultured at 37°C in 5% $CO_2$. The medium was replaced every 2 days. When the cultures reached 90% confluence, cells were passaged and re-plated in 150-$cm^2$ flasks (Corning, Big Flats, NY, USA).

Bone marrow stromal cells were obtained by iliac aspiration from three male volunteers (ages [yrs] 29, 33, 48), and were seeded in flasks and maintained in serum-conditioned α-MEM. The following day, floating cells were removed, and the medium was replaced with fresh medium. Passages were performed when cells reached 90% confluence. To ensure phenotypic uniformity, we used each cell lineage at the same passage (from 2 to 6) in the subsequent experiments.

## Pre-treatment with Basic FGF

Cells were pre-treated with bFGF under conditions described elsewhere (Fakhry *et al.*, 2005), with modifications. Both cell types were cultured in serum-conditioned α-MEM in dishes to 60% confluence. At that point, the serum-conditioned α-MEM was replaced with medium containing 1 ng/mL recombinant human bFGF (donated by Professor Y. Tabata, Kyoto University, Kyoto, Japan) and 100 μM ascorbic acid (Wako, Osaka, Japan), and the cells were cultured for 2 more days. Then, the cells were detached with trypsin-EDTA and re-plated (FGF pre-treatment).

## Cell Proliferation Assay

On day 0, each cell type was plated at a density of 2.0 x $10^4$ cells/mL/well in 12-well plates (Greinerbio-one, Kremsmuenster, Austria) containing serum-conditioned α-MEM. Cell numbers were counted directly in triplicate, and the medium was replaced with fresh serum-conditioned α-MEM on days 1 and 3.

## Alkaline Phosphatase Activity Assay

On day 0, both cell types (with and without bFGF pre-treatment) were plated at a density of 1.0 x $10^5$ cells/mL/well in 12-well plates containing serum-conditioned α-MEM. On day 1, either 1, 5, or 10 ng/mL bFGF or 30, 100, or 300 ng/mL recombinant human BMP-2 (donated by Astellas Pharma Inc., Tokyo, Japan) was added to each well, along with 100 μM ascorbic acid. On day 4, the medium was replaced with fresh medium containing identical growth factors. On day 7, cells were harvested and extracted with 20 mM HEPES (Dojindo, Kumamoto, Japan) buffer (pH 7.5) containing 1% Triton X-100 (Wako). Alkaline-phosphatase-specific (ALP) activity was assayed as described previously (Asahina *et al.*, 1993). ALP activity is expressed as μmol p-nitrophenol/min/μg protein.

## Reverse-transcription/Polymerase Chain-reaction

For RNA preparation, on day 0, both cell types (with and without FGF pre-treatment) were plated in 10-cm dishes containing serum-conditioned α-MEM. Cells were treated with or without 100 ng/mL BMP-2, 100 μM ascorbic acid for the following 6 days. Media were completely replaced on days 1 and 4. On day 7, total RNA was extracted with the use of TRIZOL reagent (Invitrogen). RNA samples (1 μg) were reverse-transcribed with Superscript III® reverse-transcriptase and oligo-dT primers (Invitrogen), according to the manufacturer's protocol. For PCR amplification, we used primer sequences that have been described previously (Wordinger *et al.*, 2002; Kamata *et al.*, 2004). We analyzed gene expression of glyceraldehyde-3′-phosphate dehydrogenase (GAPDH), type I collagen (Col I), ALP, osteopontin (OP), osteocalcin (OC), BMP-2, BMP-4, and BMP receptors (BMPr) IA, IB, and II. After amplification, samples were analyzed by electrophoresis on a 1.5% agarose gel, and were visualized by ethidium bromide staining.

## Transplantation of Cells into Immunodeficient Mice

For each transplantation, 1 x $10^6$ harvested cells (with or without pre-treatment), in 1 mL of serum-conditioned α-MEM, were mixed with 50 mg of β-tricalcium phosphate (β-TCP) granules (Osferion®; Olympus, Tokyo, Japan) in a 14-mL polypropylene tube (Becton Dickinson, Franklin Lakes, NJ, USA). For the ensuing 6 days, cells were cultured in media with 100 ng/mL BMP-2 and 100 μM ascorbic acid, or without these additives as a control. The medium was replaced with fresh identical medium on day 4. After culture, each cell mixture was transplanted into a 6-week-old female BALB/cAJcl-nu/nu mouse (Nihoncrea, Tokyo, Japan). Five subcutaneous pockets were created in the back of each mouse, under anesthesia with diethyl ether, and the cell mixture was transplanted. As a negative control, β-TCP alone was prepared and implanted into the mice. The transplants were harvested after 4 wks. NIH guidelines for the care and use of laboratory animals were observed in all procedures.

## Histomorphometric Analysis of the Transplants

The harvested samples were fixed in 4% formaldehyde, decalcified, and embedded in paraffin wax. Then, 5-μm-thick sections were prepared from the middle of each transplant and

stained with hematoxylin and eosin. The volume of newly formed bone was analyzed with Scion Image software (NIH, Bethesda, MD, USA), as described previously (Alsberg *et al.*, 2001); the bone area is expressed as the percentage of total area (27.2 $mm^2$).

### Statistical Analysis

Results are expressed as mean values ± standard deviation. Statistical analysis of differences between groups was performed with Student's *t* test.

## RESULTS

### Cell Proliferation

Proliferation of periosteal cells was significantly greater than that of bone marrow stromal cells (Fig. 1a). Although the number of periosteal cells was similar to that of marrow stromal cells on day 1, periosteal cells were twice as numerous as marrow stromal cells on day 3. Periosteal cells proliferated much faster than did marrow stromal cells, and had reached 100% confluence by day 6. Up to and including passage 6, all periosteal cells (regardless of donor) proliferated faster than the fastest-proliferating marrow stromal cells; in later passages, both cell types proliferated slightly slower (data not shown). FGF-pre-treated periosteal cells proliferated slightly slower than non-pre-treated periosteal cells (Fig. 1b), but they still proliferated faster than marrow stromal cells.

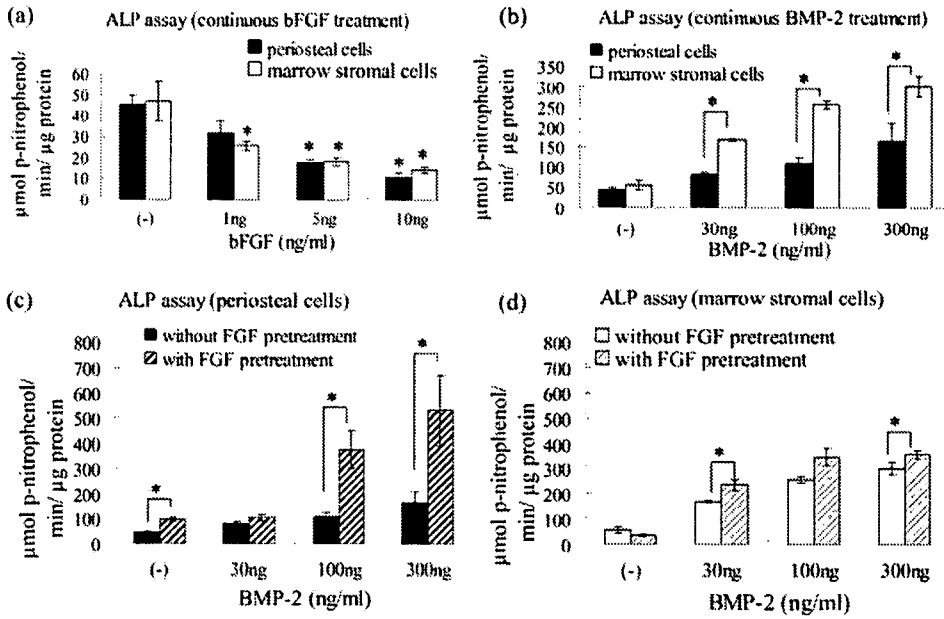


**Figure 2.** Periosteal cells (black) and marrow stromal cells (white) were plated in 12-well plates at a density of 1.0 x $10^5$ cells/well. Then, the cells were incubated with bFGF (**a**) or BMP-2 (**b**) for 6 days. Alkaline phosphatase activity was analyzed on day 7 of culture. In (a), asterisk indicates significant difference ($p < 0.05$), compared with the control (-). FGF-pre-treated periosteal cells are indicated by black hatched bars; non-pre-treated periosteal cells are indicated by black bars; FGF-pre-treated marrow stromal cells are indicated by white hatched bars; non-pre-treated marrow stromal cells are indicated by white bars (**c,d**). Values are means ± standard deviation for 3 cultures. In b-d, asterisk indicates significant difference ($p < 0.05$) between paired conditions.

### Alkaline Phosphatase Activity

Recombinant human bFGF had an inhibitory effect on ALP activity in both cell types, in a dose-dependent manner. Continuous exposure to bFGF (6 days) did not induce osteogenic differentiation in either cell type (Fig. 2a). Treatment with BMP-2 significantly enhanced the ALP activity of marrow stromal cells, but did not enhance the ALP activity of periosteal cells (Fig. 2b). FGF pre-treatment enhanced the responsiveness of periosteal cells to BMP-2; at doses of 100 and 300 ng/mL BMP-2, the ALP activity of FGF-pre-treated cells was about 3 times higher than that of the non-pre-treated cells (Fig. 2c). This effect of FGF pre-treatment on the BMP-2 induced increase in ALP activity was weaker for bone marrow cells than for periosteal cells (Fig. 2d).

### Reverse-transcription/Polymerase Chain-reaction Assay

Gene expression of periosteal cells and marrow stromal cells was examined by RT-PCR (Fig. 3). Control periosteal cells expressed only Col I and GAPDH. Treating periosteal cells with BMP-2 enhanced their expression of ALP, OP, BMP2, BMP4, BMPrIA, BMPrIB, and BMPrII. FGF pre-treatment of periosteal cells enhanced their expression of ALP, OP, BMP2, BMP4, BMPrIA, and BMPrIB. Combined FGF pre-treatment and BMP-2 treatment of periosteal cells enhanced their expression of ALP, BMP2, BMP4, BMPrIA, BMPrIB, and BMPrII.

Control marrow stromal cells expressed Col I, GAPDH,

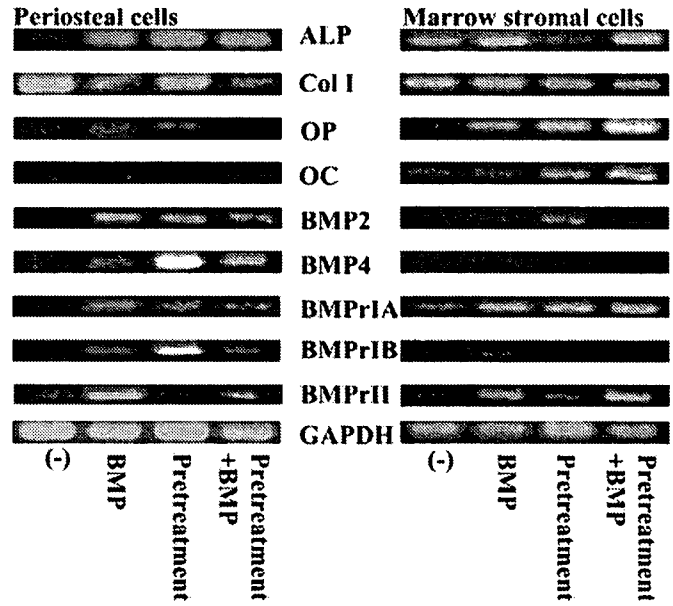


**Figure 3.** RT-PCR analysis of periosteal cells and marrow stromal cells. For 6 days, each cell type was cultured in serum-conditioned α-MEM alone (-) or in serum-conditioned α-MEM containing BMP-2 (BMP). To evaluate the effect of FGF pre-treatment, we pre-treated some cells with bFGF for 2 days (Pre-treatment), and treated some cultures with BMP after bFGF pre-treatment (Pre-treatment + BMP).

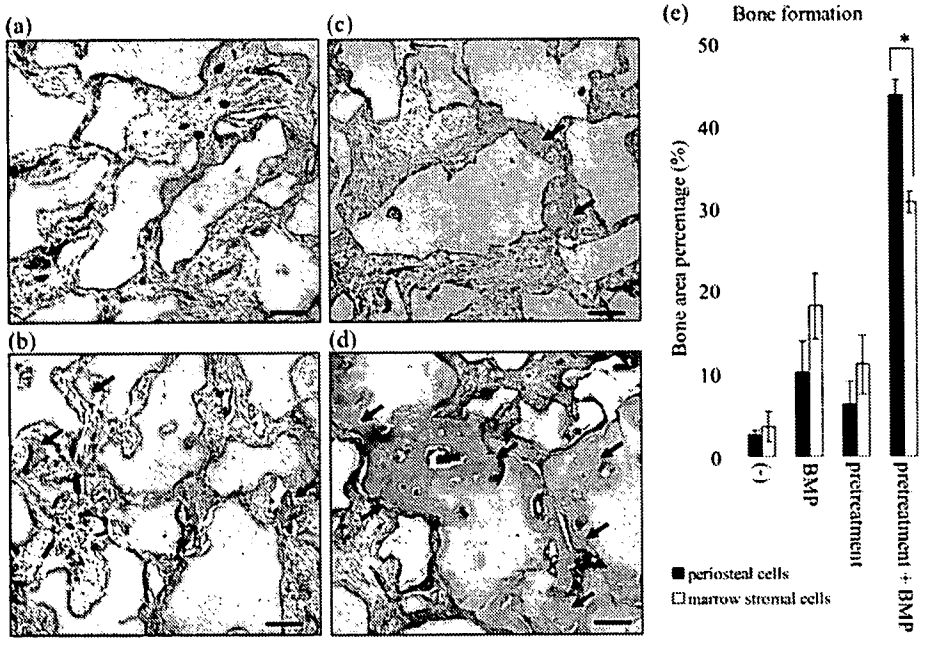


**Figure 4.** Hematoxylin and eosin staining demonstrating *in vivo* bone formation. Transplants of untreated control periosteal cells (-) formed little bone (**a**). Transplants of periosteal cells that received BMP-2 treatment alone (BMP) (**b**) or received FGF pre-treatment alone (pre-treatment) (**c**) also formed new bone. Periosteal cells that were treated with BMP-2 after FGF pre-treatment (pre-treatment + BMP) formed significant amounts of new bone (**d**). Bar indicates 300 μm. Arrow indicates new bone. The difference in new bone volume between periosteal cells (black) and marrow stromal cells (white) was determined by histomorphometric analysis (**e**). Asterisk indicates significant difference ($p < 0.05$) between paired conditions. Values are means ± standard deviation for 3 sections of each sample.

ALP, OC, BMPrIA, and BMPrII. Treating marrow stromal cells with BMP-2 enhanced their expression of ALP, OP, BMPrIA, BMPrIB, and BMPrII. FGF pre-treatment of marrow stromal cells enhanced their expression of OP, OC, BMP2, BMPrIA, and BMPrII, but it inhibited their expression of ALP. Combined FGF pre-treatment and BMP-2 treatment of marrow stromal cells enhanced their expression of ALP, OP, OC, BMP2, BMPrIA, and BMPrII.

### Transplantation of Periosteal Cells

Control periosteal cells had formed little new bone at 4 wks after transplantation (Fig. 4a). Implantation of β-TCP alone did not cause formation of any new bone (data not shown). Periosteal cells treated with BMP-2 alone or FGF pre-treatment alone also formed new bone (Figs. 4b, 4c); however, the amount of newly formed bone was less than that of periosteal cells treated with BMP-2 after FGF pre-treatment. Periosteal cells treated with BMP-2 after FGF pre-treatment had formed significant ectopic new bone at 4 wks after transplantation (Fig. 4d).

Histomorphometric analysis showed that marrow stromal cells formed slightly more new bone than did periosteal cells under control conditions (untreated), after treatment with BMP-2 alone, and after FGF pre-treatment alone; however, these differences were not statistically significant. Periosteal cells treated with BMP-2 after FGF pre-treatment generated significantly more newly formed bone than did marrow stromal cells treated with BMP-2 after FGF pre-treatment. Periosteal cells treated with BMP-2 after FGF pre-treatment formed 3 times as much new bone as did periosteal cells treated with BMP-2 without FGF pre-treatment (Fig. 4f).

## DISCUSSION

In this study, we compared the osteogenic potential and clinical usefulness of periosteal cells with those of marrow stromal cells.

The proliferation rate of periosteal cells was much greater than that of marrow stromal cells (Fig. 1a). Reports indicate that primary cultures of human bone cells obtained from different donors can have very different proliferation rates (Im *et al.*, 2004). We observed differences in proliferation rate among the present donors, but all of the present periosteal cells proliferated faster than did the present marrow stromal cells. Also in the present study, both cell types retained high expansion potential at later passages (Sakaguchi *et al.*, 2005). Thus, the use of periosteal cells may shorten the cell culture period, thereby reducing both cost and the risk of contamination.

In the present study, we used periosteal cells obtained from young adults. Aging reportedly affects the mitogenic activity of osteoprogenitor cells (Tanaka *et al.*, 1999). There is a need for studies comparing the bone-forming ability of periosteal cells between old and young donors.

Many *in vitro* studies have indicated that bFGF has a mitogenic effect on osteoprogenitor cells (Tanaka *et al.*, 1999; Shimoaka *et al.*, 2002). In contrast, the present transient bFGF treatment inhibited the proliferation of periosteal cells, although the effect was not statistically significant (Fig. 1b). The discrepancy between these studies may be due to the method of FGF treatment. In previous studies, the bFGF treatment was of longer duration than in the present study. Cells committed to the osteoblast lineage have been found to have lower proliferative potential than uncommitted cells (Malaval *et al.*, 1999). Although the present continuous treatment with bFGF inhibited ALP activity (Fig. 2a), consistent with results from a previous study (Kalajzic *et al.*, 2003), cessation of bFGF treatment may induce osteoblastic differentiation of periosteal cells. This hypothesis is consistent with the present data regarding osteoblastic gene expression of cells pre-treated with FGF. FGF pre-treatment increased the expression of molecules considered early-stage markers of osteogenic differentiation, such as ALP (Fig. 3) (Ryoo *et al.*, 2006).

BMP-2 and bFGF have been found to induce osteogenic differentiation (Canalis *et al.*, 1988; Yamaguchi *et al.*, 1991), but, in the present study, the response to BMP-2 was greater for marrow stromal cells than for periosteal cells. Control periosteal cells showed less ALP activity and expressed fewer osteogenic markers than control marrow stromal cells. This

suggests that marrow stromal cells are further differentiated along the osteoblastic cell lineage than are periosteal cells. Previous studies indicated that transient treatment with FGF, followed by treatment with BMP-2, enhanced osteogenic differentiation *in vitro* (Hanada *et al.*, 1997; Fakhry *et al.*, 2005). Similarly, in the present study, FGF pre-treatment enhanced responsiveness to BMP-2, and this enhancement was much stronger in periosteal cells than in marrow stromal cells. This suggests that the enhancement of osteogenic potential after FGF pre-treatment was due to an increase in the number of cells in the pre-osteoblast or osteoblast lineage.

Consistent with previous *in vitro* studies, the present combination of FGF pre-treatment and BMP-2 treatment enhanced the bone-forming potential of periosteal cells, which formed a greater volume of new bone than did marrow stromal cells *in vivo*. Thus, periosteal cells cultured under conditions that promote osteogenesis may be as useful for bone tissue engineering as are marrow stromal cells, and offer the advantage of greater proliferation.

## ACKNOWLEDGMENTS

This study was supported by a Grant-in-aid for Scientific Research (No. 16659547) from the Japan Society for the Promotion of Science, and by Grants-in-aid from Hitachi Medical Corporation (Japan) and Denix International Corporation (Japan).

## REFERENCES

Alsberg E, Anderson KW, Albeiruti A, Franceshi RT, Mooney DJ (2001). Cell-interactive alginate hydrogels for bone tissue engineering. *J Dent Res* 80:2025-2029.

Asahina I, Sampath TK, Nishimura I, Hauschka PV (1993). Human osteogenic protein-1 induces both chondroblastic and osteoblastic differentiation of osteoprogenitor cells derived from newborn rat calvaria. *J Cell Biol* 123:921-933.

Breitbart AS, Grande DA, Kessler R, Ryaby JT, Fitzsimmons RJ, Grant RT (1998). Tissue engineered bone repair of calvarial defects using cultured periosteal cells. *Plast Reconstr Surg* 101:567-574.

Canalis E, Centrella M, McCarthy T (1988). Effects of basic fibroblast growth factor on bone formation *in vitro*. *J Clin Invest* 81:1572-1577.

Fakhry A, Ratisoontorn C, Vedhachalam C, Salhab I, Koyama E, Leboy P, *et al.* (2005). Effects of FGF-2/-9 in calvarial bone cell cultures: differentiation stage-dependent mitogenic effect, inverse regulation of BMP-2 and noggin, and enhancement of osteogenic potential. *Bone* 36:254-266.

Hanada K, Dennis JE, Caplan AI (1997). Stimulatory effects of basic fibroblast growth factor and bone morphogenetic protein-2 on osteogenic differentiation of rat bone marrow-derived mesenchymal stem cells. *J Bone Miner Res* 12:1606-1614.

Haynesworth SE, Goshima J, Goldberg VM, Caplan AI (1992). Characterization of cells with osteogenic potential from human marrow. *Bone* 13:81-88.

Im GI, Qureshi SA, Kenny J, Rubash HE, Shanbhag AS (2004). Osteoblast proliferation and maturation by bisphosphonates. *Biomaterials* 25:4105-4115.

Kalajzic I, Kalajzic Z, Hurley MM, Lichtler AC, Rowe DW (2003). Stage specific inhibition of osteoblast lineage differentiation by FGF2 and noggin. *J Cell Biochem* 88:1168-1176.

Kamata N, Fujimoto R, Tomonari M, Taki M, Nagayama M, Yasumoto S (2004). Immortalization of human dental papilla, dental pulp, periodontal ligament cells and gingival fibroblasts by telomerase reverse transcriptase. *J Oral Pathol Med* 33:417-423.

Luria EA, Owen ME, Friedenstein AJ, Morris JF, Kuznetsow SA (1987). Bone formation in organ cultures of bone marrow. *Cell Tissue Res* 248:449-454.

Malaval L, Liu F, Roche P, Aubin JE (1999). Kinetics of osteoprogenitor proliferation and osteoblast differentiation in vitro. *J Cell Biochem* 74:616-627.

Marie PJ (2003). Fibroblast growth factor signaling controlling osteoblast differentiation. *Gene* 316:23-32.

Matsubara T, Suardita K, Ishii M, Sugiyama M, Igarashi A, Oda R, *et al.* (2005). Alveolar bone marrow as a cell source for regenerative medicine: differences between alveolar and iliac bone marrow stromal cells. *J Bone Miner Res* 20:399-409.

Perka C, Schultz O, Spitzer RS, Lindenhayn K, Burmester GR, Sittinger M (2000). Segmental bone repair by tissue-engineered periosteal cell transplants with bioresorbable fleece and fibrin scaffolds in rabbits. *Biomaterials* 21:1145-1153.

Rosen V, Thies RS (1992). The BMP proteins in bone formation and repair. *Trends Genet* 8:97-102.

Ryoo HM, Lee MH, Kim YJ (2006). Critical molecular switches involved in BMP-2-induced osteogenic differentiation of mesenchymal cells. *Gene* 366:51-57.

Sakaguchi Y, Sekiya I, Yagishita K, Muneta T (2005). Comparison of human stem cells derived from various mesenchymal tissues: superiority of synovium as a cell source. *Arthritis Rheum* 52:2521-2529.

Shimoaka T, Ogasawara T, Yonamine A, Chikazu D, Kawano H, Nakamura K, *et al.* (2002). Regulation of osteoblast, chondrocyte, and osteoclast functions by fibroblast growth factor (FGF)-18 in comparison with FGF-2 and FGF-10. *J Biol Chem* 277:7493-7500.

Tanaka H, Ogasa H, Barnes J, Liang CT (1999). Actions of bFGF on mitogenic activity and lineage expression in rat osteoprogenitor cells: effect of age. *Mol Cell Endocrinol* 150:1-10.

Wordinger RJ, Agarwal R, Talati M, Fuller J, Lambert W, Clark AF (2002). Expression of bone morphogenetic proteins (BMP), BMP receptors, and BMP associated proteins in human trabecular meshwork and optic nerve head cells and tissues. *Mol Vis* 8:241-250.

Yamaguchi A, Katagiri T, Ikeda T, Wozney JM, Rosen V, Wang EA, *et al.* (1991). Recombinant human bone morphogenetic protein-2 stimulates osteoblastic maturation and inhibits myogenic differentiation in vitro. *J Cell Biol* 113:681-687.

Young CS, Abukawa H, Asrican R, Ravens M, Troulis MJ, Kaban LB, *et al.* (2005). Tissue-engineered hybrid tooth and bone. *Tissue Eng* 11:1599-1610.

Cytotechnology (2005) 47:127–131
DOI 10.1007/s10616-005-3749-4



*Short Communication*

# Relations between individual cellular motions and proliferative potentials in successive cultures of human keratinocytes

Norihiko Hata[1], Yuka Agatahama[1], Masahiro Kino-oka[1] and Masahito Taya[1,2,*]
*[1]Division of Chemical Engineering, Graduate School of Engineering Science, Osaka University, 1-3 Machikaneyama-cho, Toyonaka, Osaka 560-8531, Japan; [2]Graduate School of Frontier Biosciences, Osaka University, 1-3 Machikaneyama-cho, Toyonaka, Osaka 560-8531, Japan; *Author for correspondence (e-mail: taya@cheng.es.osaka-u.ac.jp; phone: +81-06-6850-6251; fax: +81-06-6850-6254)*

Received 5 March 2004; accepted as revised form 15 May 2005

*Key words:* Cell extension, Cell rotation, Doubling time, Human keratinocytes, Lag time, Motion analysis

**Abstract**

In the successive cultures of human keratinocyte cells, cellular motions of extension and rotation were analyzed based on observation of the individual cells, to evaluate the proliferative potential in a whole cell population. In lag phases of the serial cultures, an extension index of individual cells, $R_E$, was defined as an average spreading rate divided by initial cell area for each cell. The mean value of $R_E$ was found to relate to prolongation of lag time; namely it decreased with increasing passage number in the successive cultures approaching cellular senescence. During the courses of the cultures, the rotation rate of paired cells was also measured through time-lapse observation. The mean value of rotation rate, $|\bar{\omega}|$, decreased with an increase in doubling time caused by the progress of cellular age, reaching an almost constant value of $|\bar{\omega}| = 40$ degrees $h^{-1}$ in the cultures with prolonged doubling time of over 59 h. It was concluded that the indices determined from the motions of individual cells, $R_E$ and $|\bar{\omega}|$, were correlated with the lag time and doubling time, respectively, which are growth parameters varied with the vitality of the cells approaching cellular senescence.

*Nomenclature:* $A_C$ – projected area of each cell ($\mu m^2$); $A_{C0}$ – initial projected area of each cell ($\mu m^2$); $n$ – number of examined cells (cells); $N_d$ – cumulative number of population doublings; $N_{df}$ – final value of cumulative number of population doublings; $N_P$ – number of passages; $r_s$ – spreading rate of each cell ($\mu m^2\ h^{-1}$); $r_s^{ave}$ – average spreading rate of each cell ($\mu m^2\ h^{-1}$); $R_E$ – cell extension index ($h^{-1}$); $\bar{R}_E$ – mean value of $R_E$ ($h^{-1}$); $t$ – observation time (h); $t_d$ – doubling time (h); $t_L$ – lag time (h); $|\omega|$ – absolute value of rotation rate (degree $h^{-1}$); $|\bar{\omega}|$ – mean value of $|\omega|$, (degree $h^{-1}$)

## Introduction

For the production of cultured tissues such as epithelial sheets, a series of monolayer cultures of anchorage-dependent cells is generally performed to expand cell number requisite for tissue reconstruction. In these cultures, the natures of source cells are of heterogeneity depending on the respective biopsies from which the cells are isolated, and the vitality of cell individuals progressively lowers due to cellular senescence inherent in normal human cells.

From a viewpoint of growth kinetics of anchorage-dependent cells, lag time and doubling time are

important parameters to estimate the cell vitality or activity. In a lag phase, cells extend with morphological alternation to ensure firm adhesion onto culture surface, giving a delay in cell growth, lag time, that changes with culture conditions and/or cell states (Re et al. 1994). In a subsequent growth phase, cells generate their daughters through repeated cell division at an interval of generation time, relying on multiplying ability of each cell.

In previous work (Hirai et al. 2002; Kino-oka et al. 2004), we developed the culture system which facilitated the direct observation of dynamic behaviors of individual cells. It was demonstrated that the spreading rate of each cell found in lag phase could be a criterion for estimating time until the first cell division in the culture of murine fibroblasts prepared under varied conditions of trypsin treatment. Moreover, the rotation rate of paired cells was proposed to evaluate the vitality or latent potential of growth recovery in the culture of human immortal epithelial cells kept under glucose-limited conditions. The aim of the present study is to extend the motion analyses of cell spreading and rotation to evaluating the proliferative potential in the successive cultures of normal human keratinocytes. The growth potential parameters of lag time and doubling time that change with the progress of cellular age will be discussed in terms of the proposed indices determined from observing the dynamic behaviors of individual cells.

## Materials and methods

Human keratinocytes (neonatal foreskin origin) were obtained as frozen cells from Kurabo Ind., Osaka, Japan (No.9C0708 in supplier's file). The cells in vials were thawed according to the supplier's instruction, and then cultivated in a 25 $cm^2$ T-flask (Nunclon Delta Flask; Nunc, Roskilde, Denmark) as the first passage ($N_P$ = 1) in a series of successive cultures. The cultures were conducted using serum-free medium (HuMedia-KG2; Kurabo Ind., Osaka, Japan) at 37°C under air containing 5% $CO_2$. The medium was maintained at a depth of 4 mm in the flask and spent medium was renewed every 3 days. On reaching about 80% confluence of the cells on the flask bottom, the cells were harvested by centrifugation ($200 \times g$, 25°C) after enzymatic treatment with a mixture of 0.1% trypsin 1:250 and 0.02% EDTA (Sigma Aldrich, St. Louis, MO, USA). The subsequent passages were repeated in a similar manner until the cell growth substantially ceased. In these successive cultures, the initial concentration of viable cells, determined by trypan blue exclusion test, was fixed at $1.0 \times 10^4$ cells/$cm^2$. Throughout the experiments, all the cultures for the data analyses were carried out in triplicate. During each passage, the remaining number of population doublings, $N_{df}-N_d$, was determined as a measure for cellular senescence, based on the change of adherent cell concentration as shown elsewhere (Umegaki et al. 2002).

As described in a previous study (Kino-oka et al. 2004), an observation tool was constructed by installing a CCD camera in the computer-aided culture system and employed to analyze individual cellular motions during the courses of the cultures. The cell images were captured in a manner of time-lapse observation, every 40 min for 10 h in an early lag phase and every 20 min for 24 h in an early growth phase, for analyzing cell spreading rate and paired cells rotation, respectively, at five positions in each flask. Table 1 indicates the values of $N_P$ and $N_{df}-N_d$ during the successive cultures of keratinocytes (Runs 1–3) employed for the observation of these cellular motions.

## Results and discussion

To analyze the spreading rate of the keratinocyte cells, the projected area of each cell, $A_C$, in lag phase was determined by extracting cellular edge using a line-drawing tool in the software (IMAQ Vision Builder; National Instruments, Austin, TX, USA). The $A_C$ values of individual cells increased

*Table 1.* Values of $N_P$ and $N_{df}-N_d$ in successive cultures of keratinocyte cells used for experiments.

| Culture | $N_P$ [–] | $N_{df}-N_d$ [–] |
|---|---|---|
| Run 1 | 3 | 6.6 to 9.6 |
| | 4 | 3.8 to 6.6 |
| | 5 | 0.9 to 3.8 |
| | 6 | 0 to 0.9 |
| Run 2 | 4 | 3.5 to 6.8 |
| | 5 | 0.9 to 3.5 |
| | 6 | 0 to 0.9 |
| Run 3 | 5 | 2.7 to 5.8 |
| | 6 | 0.1 to 2.7 |
| | 7 | 0 to 0.1 |

gradually with elapsed time after seeding. Then the spreading rate of each cell, $r_s = dA_C/dt$, was traced and an average $r_s$ of values, $r_s^{ave}$, was determined in each culture. The determined $r_s^{ave}$ value was standardized in terms of initial cell area, $A_{C0}$, to define a cell extension index, $R_E$, as follows.

$$R_E = r_s^{ave}/A_{C0} \quad (1)$$

Figure 1 shows the histograms of $R_E$ values of the examined cells during the successive cultures (Run 1). In the culture of $N_P = 3$, a broad distribution in the $R_E$ values was recognized, ranging from $R_E = 0.04$ to $0.30\ h^{-1}$. Afterwards, the distribution shifted to small values with an increase in the $N_P$ value. The frequency of cells with $R_E < 0.10\ h^{-1}$ was approximately 80% in the culture of $N_P = 6$ with $N_{df}-N_d = 0$ to 0.9 as

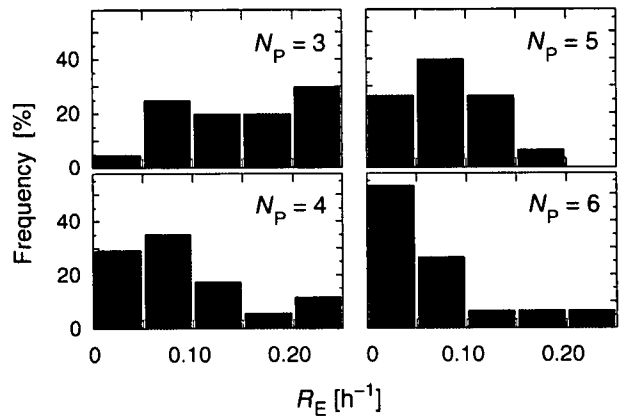


*Figure 1.* Histograms of cell extension index, $R_E$, in successive cultures of keratinocyte cells (Run 1). The $R_E$ values were determined for early 10 h in each culture ($n$ = 15 to 20 cells).

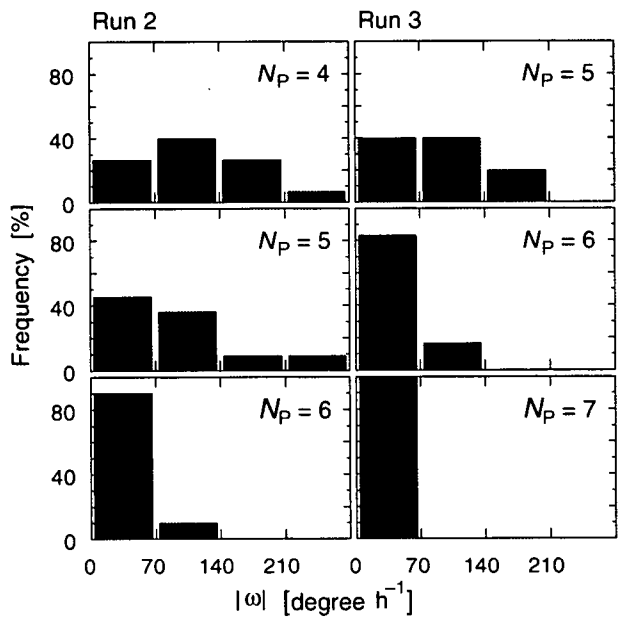


*Figure 2.* Histograms of rotation rate, $|\omega|$, in successive cultures of keratinocyte cells (Runs 2 and 3). The $|\omega|$ values were determined for 1 h form $t$ = 24 h in each culture ($n$ = 5 to 15 cells).

shown in Table 1, and its frequency pattern was different from that in the culture of $N_P$ = 3 with $N_{df}$–$N_d$ = 6.6 to 9.6 ($p < 0.05$). These results indicated that the extension potential of the keratinocyte cells in lag phase deteriorated in response to the progress of cellular age, as evaluated by the $N_{df}$–$N_d$ value.

Next, the rotation of paired cells was observed by capturing cell images during the successive cultures of the keratinocyte cells (Runs 2 and 3). This pairwise rotation was quantified as an absolute value of rotation rate, $|\omega|$, which was determined according to the procedure reported earlier (Kino-oka et al. 2004). Figure 2 shows the histograms of the $|\omega|$ values of the examined cells during the successive cultures. In the culture of $N_P$ = 4 (Run 2), a broad distribution in the $|\omega|$ values was observed in the range of $|\omega|$= 4 to 254 degrees $h^{-1}$, which indicated that the culture comprised of heterogeneous population of cells with varied rotational motions. With an increase in the passage number, the distribution in the $|\omega|$ value narrowed and almost the cells entered a region of $|\omega| < 70$ degrees $h^{-1}$ in the culture of $N_P$ = 6 with $N_{df}$–$N_d$ = 0 to 0.9 (see Table 1). A similar tendency was also recognized in the separately conducted successive cultures (Run 3).

Then we intended to correlate these cellular motions of extension and rotation with proliferative potentials of cell population in the successive cultures. As indices for the proliferative potentials of cell population, lag time, $t_L$, and doubling time, $t_d$, were determined from the growth profile of cells in each passage as described in previous work (Kino-oka et al. 2000). Figure 3a shows the plot of the mean $\bar{R}_E$, value, $\bar{R}$ against lag time in the

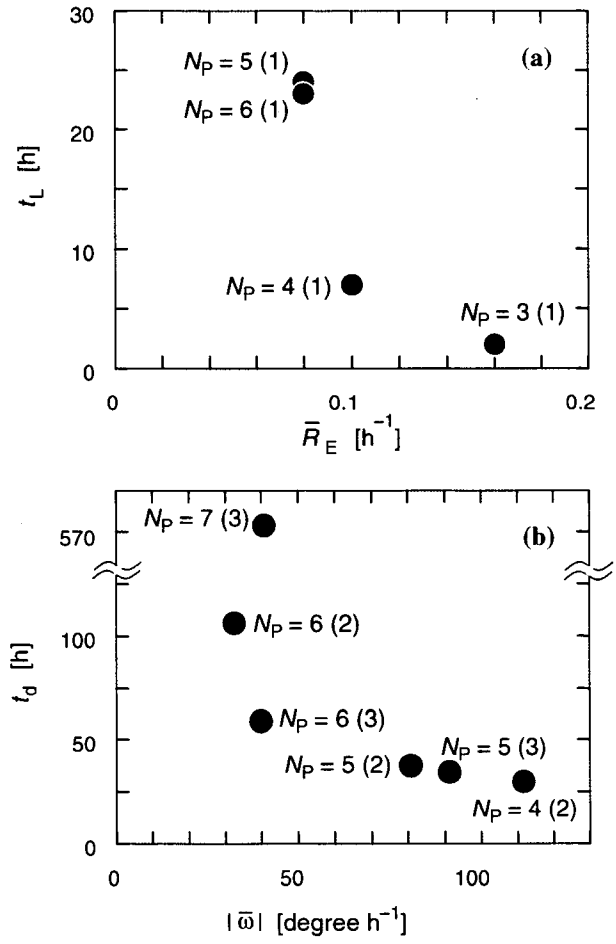


*Figure 3.* Plots of (a) mean $R_E$ value, $\bar{R}$, against lag time, $t_L$, and (b) mean $|\omega|$ value, $|\bar{\omega}|$, against doubling time, $t_d$, in successive cultures of keratinocyte cells. The numerals in the parentheses indicate run number.

successive cultures (Run 1). In these cultures, the cells exhibited substantial proliferation with $t_d$ = 17.3, 26.5 and 33.2 h, respectively, at $N_P$ = 3, 4 and 5, while the $t_d$ value extremely prolonged up to 82.2 h at $N_P$ = 6. As seen in Figure 3a, lag time elongated along with decreasing $\bar{R}$ from 0.16 to 0.08 $h^{-1}$ and reached $t_L \cong 23$ h at the last two passages of the successive cultures ($N_P$ = 5 and 6). This result suggests that cellular senescence causes the deterioration of adhesive potential of anchorage-dependent cells, including the attachment and extension of the cells on culture surface that are critical events in lag phase to render the cells ready for cell division in growth phase, as pointed out in a literature (Gumbiner 1996).

Figure 3b shows the relation between the mean value of $|\omega|$, $|\bar{\omega}|$, and doubling time of the cells in each passage of the keratinocyte cultures. The $|\bar{\omega}|$ value was at low levels of 30–40 degrees $h^{-1}$ in a region of $t_d$ = 59 to 573 h ($N_P$ = 6 and 7), and it exhibited a gradual increase with shortening $t_d$ value observed in the early passages ($N_P$ = 4 and 5), indicating that the growth potential is high in the culture containing the cells with the elevated rotation rate. It was thus demonstrated that the rotational motion of the cells can be a parameter to evaluate the multiplying ability of the anchorage-dependent cells.

In conclusion, the individual cellular motions of extension and pairwise rotation were examined in the successive cultures of keratinocytes associated with the progress of cellular age. The indices determined from the motions of individual cells, $R_E$ and $|\omega|$, were correlated with the conventional proliferative potentials estimated from a whole cell population, lag time and doubling time, respectively. The cellular motion analyses based on observing cell individuals can offer useful tools to know the state of the cells approaching cellular senescence along with the serial passages encountered in the culture of normal human cells.

## Acknowledgement

The authors thank Miss S. Gondo for her assistance in a part of experiments.

## References

Gumbiner B.M. 1996. Cell adhesion: the molecular basis of tissue architecture and morphogenesis. Cell 84: 345–357.

Hirai H., Umegaki R., Kino-oka M. and Taya M. 2002. Characterization of cellular motions through direct observation of individual cells at early stage in anchorage-dependent culture. J. Biosci. Bioeng. 94: 351–356.

Kino-oka M., Agatahama Y., Hata N. and Taya M. 2004. Evaluation of growth potential of human epithelial cells by motion analysis of pairwise rotation under glucose-limited condition. Biochem. Eng. J. 19: 109–117.

Kino-oka M., Umegaki R., Taya M., Tone S. and Prenosil J.E. 2000. Valuation of growth parameters in monolayer keratinocyte cultures based on a two-dimensional cell placement model. J. Biosci. Bioeng. 89: 285–287.

Re F., Zanetti A., Sironi M., Polentarutti N., Lanfrancone L., Dejana E. and Colotta F. 1994. Inhibition of anchorage-dependent cell spreading triggers apoptosis in cultured human endothelial cells. J. Cell Biol. 127: 537–546.

Umegaki R., Murai K., Kino-oka M. and Taya M. 2002. Correlation of cellular life span with growth parameters observed in successive cultures of human keratinocytes. J. Biosci. Bioeng. 94: 231–236.

# Glucose transporter mediation responsible for morphological change of human epithelial cells on glucose-displayed surface

**Mee-Hae Kim,[1] Masahiro Kino-oka,[2] Masaya Kawase,[3] Kiyohito Yagi,[4] and Masahito Taya[1,2]***

***Department of Biotechnology, Graduate School of Engineering, Osaka University, 2-1 Yamada-oka, Suita, Osaka 565-0871, Japan,[1] Division of Chemical Engineering, Graduate School of Engineering Science, Osaka University, 1-3 Machikaneyama-cho, Toyonaka, Osaka 560-8531, Japan,[2] Faculty of Pharmaceutical Sciences, Osaka-ohtani University, 3-11-1 Nishiki-ori, Tondabayashi, Osaka 584-8540, Japan,[3] and Graduate School of Pharmaceutical Sciences, Osaka University, 1-6 Yamada-oka, Suita, Osaka 565-0871, Japan[4]***

---

Running head: MORPHOLOGICAL CHANGES ON GLUCOSE-DISPLAYED SURFACE

* Corresponding author. e-mail: taya@cheng.es.osaka-u.ac.jp

phone: +81-(0)6-6850-6251 fax: +81-(0)6-6850-6254

**Abstract**

Cellular morphology is one of the important factors to coordinate cell signaling. In the present study, the morphological variation via glucose transporter (GLUT)-mediated anchoring was investigated in the cultures of human mammary epithelial cells in the presence or absence of insulin on the surfaces with the changed ratios of D- and L-glucose displayed. With increasing ratio of D-glucose displayed on the surfaces, the cells showed the stretched shape in the culture with 10 $\mu g/cm^3$ insulin, reaching the highest extent of cell stretching at 100% D-glucose display, while the round shaped cells were dominant at 0% D-glucose display. In the absence of insulin, on the other hand, the extent of cell stretching depicted a concave profile in terms of the ratio of D-glucose displayed, the extent being the highest at 50% D-glucose display. Blocking of integrin $\alpha_5\beta 1$ or GLUTs1 and 4 on the cells with corresponding antibodies revealed that the primary mechanism for cell attachment was based on integrin-mediated binding, and that GLUTs1 and 4 contributed largely to morphological changes of cells. In confocal microscopic examination, moreover, it was found that GLUT4 localization occurred in response to the D-glucose display as well as insulin addition. In the absence of insulin, GLUT4 spots were extensively observed in cell body whether the D-glucose was displayed or not. However, in the presence of insulin, the broad distribution of GLUT4 appeared on the basal and apical sides of cells at 100% D-glucose display, in contrast with its localization only on the apical cell side at 0% D-glucose display. These results suggest that the quantitative balance of GLUTs on the cytoplasmic membrane and D-glucose displayed on the surface determines the cell morphology, as explained by a "receptor saturation" model.

**Key words:** human epithelial cells, glucose-displayed surface, glucose transporter-mediated anchoring, morphological change, cellular roundness, receptor saturation model

# INTRODUCTION

In cultures of anchorage-depending mammalian cells, adhesion-promoting proteins of extracelluar matrix (ECM), such as fibronectin and vitronectin, are complex multifunctional elements which interact with other matrix molecules and also with cytoplasmic receptors. In general, the attachment of cells onto a surface is initiated by mediation of trans-membrane receptors, mainly integrins, associated with cytoskeletal formation (1-3). Integrin-mediated binding on a surface leads to the formation of focal contacts through a cascade of phosphorylation events, resulting in linking the ECM proteins on the extracellular face of the cytoplasmic membrane to cytoskeletal proteins with actin filaments on the intracellular face (4, 5). Moreover, these events give rise to the recruitment and assembling of actin-binding proteins, being attributed to the stimulation of intracellular signal transduction pathways. This coordination between the integrins and their binding sites ultimately concerns the cellular fates with respect to adhesion, spreading, migration, division and differentiation (6-11).

The mechanisms of integrin-mediated changes in cell morphology have been considered to be attributed to linkages between the integrin domains on the cytoplasmic membrane (5, 6). Various elements of ECM contribute to morphological changes accompanied with variation in cytoskeletal organization. In particular, variation in the surface quantity of integrin-mediated binding sites has been demonstrated to be an important factor for morphological changes in several cell species (12). A recent technique for the regulation of surface adhesion ability of cells is the coating of RGD (Arg-Gly-Asp), which is a functional domain of fibronectin and other ECM molecules

(13, 17). This technique was extended to preparing substrates with localized ligand display. The development of these substrates for cell adhesion can provide new insights into cell biology as well as sophisticated methodology for controlling morphogenesis of cultured cells and tissues (10, 11, 16, 18).

The carbohydrate moieties have been used to mediate attachment of hepatocyte cells in the field of tissue engineering to address the asialoglycoprotein receptor as well as transporters (19-21, 22, 23). Akaike and co-workers reported that the molecular recognition between asialoglycoprotein receptor and galactose ligand resulted in specific adhesion of hepatocytes on synthetic matrix and preserved the differentiated hepatic functions by promoting the formation of round adherent cells and aggregates (24, 25). Among natural carbohydrates, glucose has been focused as a specific cell recognition molecule because it is a common source for cellular component synthesis and biological energy yielding. The passive uptake of glucose via glucose transporters (GLUTs) is necessary for mammalian cells' metabolism (26, 27), and several different GLUTs works on the cytoplasmic membranes in various kinds of cells (28).

In the previous work (29), the morphological variation was observed in cultures of rabbit chondrocyte cells on D-glucose displayed surface where the ratio of D- and L-glucose displayed was changed. To gain access to the initial cellular events on D-glucose displayed surface, in the present study, we investigate the influence of displaying D-glucose on the attachment and morphology of human epithelial cells with changed expression of GLUTs by addition of insulin. Moreover, the fundamental mechanisms of cell and culture surface interaction are discussed concerning the formation of actin cytoskeleton and binding domain.